PHYSICAL REVIEW D **78,** 094004 (2008)

Single inclusive pion p_T spectra in proton-proton collisions at $\sqrt{s} = 22.4$ GeV: Data versus perturbative QCD calculations

François Arleo[1] and David d'Enterria[2]

[1]*LAPTH*[*], *Université de Savoie, CNRS, BP 110, 74941 Annecy-le-Vieux cedex, France*

[2]*CERN, PH Department, 1211 Geneva 23, Switzerland*

(Received 8 July 2008; published 6 November 2008)

We compare the inclusive transverse momentum spectra of single pions above $p_T = 3$ GeV/c measured in proton-proton (p-p) collisions at $\sqrt{s} = 21.7$–23.8 GeV, with next-to-leading-order (NLO) perturbative QCD (pQCD) predictions using recent parametrizations of the parton densities and parton-to-pion fragmentation functions. Although the dependence on the theoretical scales is large, the calculations can reproduce the experimental results both in magnitude and shape. Based on the existing data and on a pQCD $\sqrt{s}$ rescaling of the measured spectra, we provide a practical parametrization of the baseline p-p pion transverse momentum spectrum to be compared to nucleus-nucleus collisions data at $\sqrt{s_{NN}} = 22.4$ GeV.

DOI: 10.1103/PhysRevD.78.094004 PACS numbers: 13.85.Ni, 12.38.−t, 12.38.Bx, 13.87.Fh

I. INTRODUCTION

The study of hadron production at large transverse momenta ($p_T \gg \Lambda_{\rm QCD} \approx 0.2$ GeV) in hadronic interactions is a valuable testing ground of the perturbative regime of quantum chromodynamics (pQCD), providing information on both the parton distribution functions (PDFs) in the proton and the parton-to-hadron fragmentation functions (FFs) [1]. In the past years, a renovated interest in high-p_T hadron production has been driven mainly by studies of "jet quenching" phenomena in high-energy nucleus-nucleus (A-A) collisions [2] as well as of the proton spin structure in polarized p-p collisions [3,4]. In A-A collisions, the observed large suppression of high-p_T hadron yields compared to (appropriately scaled) p-p cross sections [5,6]—attributed to parton energy loss due to medium-induced gluon radiation [7,8]—provides valuable information on the transport properties of hot and dense QCD matter [2]. The energy density at which such jet quenching phenomena sets in in A-A collisions can signal the possible transition from a hadronic to a deconfined quark-gluon system. Whereas unambiguous signals of high-p_T hadron suppression have been found at Relativistic Heavy-Ion Collider (RHIC) in central Au-Au collisions at $\sqrt{s_{NN}} = 200$ [5,6] and 62.4 GeV [9,10], one cannot draw any firm conclusion yet at Super Proton Synchrotron (SPS) energies ($\sqrt{s_{NN}} = 17.3$ GeV) [11] due to the lack of a valid (experimental and/or theoretical) proton-proton reference [12]. Recently, the PHENIX Collaboration has presented results on high-p_T neutral pion production in Cu-Cu collisions at energies $\sqrt{s_{NN}} = 22.4$ GeV, close to the SPS range [13]. We present here an experimental and theoretical study of the pion p_T spectrum in p-p collisions required in order to determine the associated nuclear "suppression factor" $R_{AA}(p_T) \propto (dN_{AA}/dp_T)/(dN_{pp}/dp_T)$ in A-A collisions at this center-of-mass (c.m.) energy.

In Sec. II, we compile and examine all existing experimental spectra for π^0 [14–21] and $\pi^{\pm}$ [21,22] at c.m. energies in the range $\sqrt{s} = 21.7$–23.8 GeV. We notice that most of the data appear to be consistent with each other within uncertainties, despite some spread. In Sec. III, we compare these data to pQCD calculations at next-to-leading order (NLO) accuracy, as implemented in the Monte Carlo program INCNLO [23,24]. We discuss in some detail the improvements in the model predictions thanks to the use of recent FFs [25]. For a choice of renormalization-factorization scales in the low side ($\mu/p_T = 1/3 - 1/2$), the calculations can reproduce the experimental results in both magnitude and shape within the uncertainties associated with the limited knowledge of the parton-to-pion FFs and PDFs in this kinematic range. Finally, a practical parametrization of the p-p pion transverse momentum spectrum at $\sqrt{s} = 22.4$ GeV is provided in Sec. IV for use as a denominator in the determination of the corresponding nuclear modification factor in A-A collisions in the low range of energies accessible at the RHIC collider.

II. INCLUSIVE PION SPECTRA IN p-p COLLISIONS AT $\sqrt{s} \approx 22.4$ GeV: EXPERIMENTAL MEASUREMENTS

Table I compiles the 13 measurements found in the literature for neutral [14–21] and charged [21,22] pion production at c.m. energies around $\sqrt{s} = 22.4$ GeV at midrapidity ($y = 0$, corresponding to laboratory angles $\theta_{\rm lab} \approx 1$ rad in fixed-target kinematics). The data were measured in the 1970s at the CERN–intersecting-storage-ring (ISR) collider as well as in the 1980s in various CERN and Fermi National Accelerator Laboratory (Fermilab) fixed-target experiments. The corresponding data points

[*]Laboratoire d'Annecy-le-Vieux de Physique Théorique, UMR5108.

TABLE I. Compilation of inclusive pion production data in p-p collisions around $\sqrt{s} = 22.4$ GeV and midrapidity: collision, center-of-mass energy, $p_{\rm lab}$ (for fixed-target experiments), collaboration/experiment name, bibliographical reference, measured p_T range, total number of data points, and associated systematic uncertainties in the measured cross sections.

Reaction	$\sqrt{s}$ (GeV)	$p_{\rm lab}/c$ (GeV)	Collab./Exp.	Ref.	p_T range (GeV/c)	# data points	Syst. uncertainties
$pp \to \pi^0 X$	21.7	250	FNAL E-063	[14]	0.7–2.4	29	30%
$pp \to \pi^- X$	21.7	250	EHS-NA22	[22]	0.1–2.2	45	···
$pp \to \pi^0 X$	22.8	275	FNAL E-063	[14]	0.4–3.8	16	30%
$pp \to \pi^0 X$	23.0	280	CERN-WA70	[15]	4.1–6.7	8	16–30%
$pp \to \pi^{\pm} X$	23.0	···	Brit.-Scand.	[21]	0.2–3.0	17	15%
$pp \to \pi^0 X$	23.0	284	FNAL E-063	[14]	0.4–4.5	14	30%
$pp \to \pi^0 X$	23.3	···	R-107	[18]	1.0–3.0	21	35%
$pp \to \pi^0 X$	23.5	···	CCRS	[19]	2.5–4.0	17	26%
$pp \to \pi^0 X$	23.6	···	ACHM	[20]	0.7–4.5	19	35%
$pp \to \pi^0 X$	23.8	300	FNAL E-063	[14]	0.4–3.7	12	30%
$pp \to \pi^0 X$	23.8	300	CERN-NA24	[16]	1.25–6.0	9	15%
$pp \to \pi^0 X$	23.8	300	FNAL-E-268	[17]	1.3–4.2	10	5%

(adding to a total of ~220) have been obtained from the Durham database [26]. Assuming isospin symmetry, the π^0 yield is the same as the $(\pi^+ + \pi^-)/2$ yield, and thus we can use both data sets to get a combined pion reference spectrum. The last column of Table I collects the propagated experimental uncertainties of the measurements as reported in the original publications. Two types of errors are often quoted: (i) those related to energy scale (p_T) uncertainties and (ii) additional systematic and/or absolute normalization (usually luminosity) errors. The p_T-scale uncertainties have been transformed into an associated absolute cross-section uncertainty assuming a local power-law distribution with exponent $n \approx 10$. We have conservatively added all quoted uncertainties in quadrature with the point-to-point errors. We note that, at variance with the π^0 spectra measured at $\sqrt{s} \approx 63$ GeV [27], there is no need to account for possible direct-γ contaminations in the oldest "nonresolved" pion spectra since, at the lower c.m. energies considered here, the prompt-photon contributions start to be significant only *above* the momentum range ($p_T \gtrsim 6\,{\rm GeV}/c$) actually reached in the experiments.

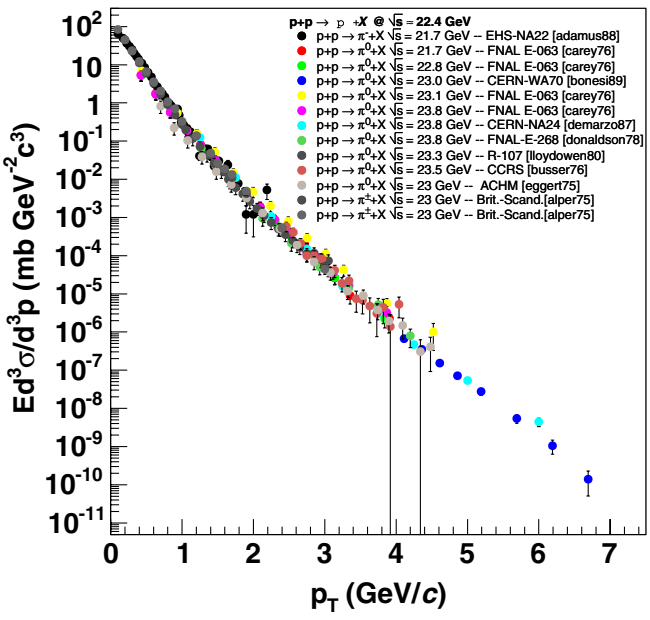

FIG. 1 (color online). Compilation of all pion transverse spectra measured in p-p collisions in the range $\sqrt{s} = 21.7$–23.8 GeV (see Table I for details).

Figure 1 shows all of the measured pion p_T spectra. The full range of cross sections covers more than 12 decades. Unlike with what was observed at $\sqrt{s} \approx 63$ GeV [27], the data taken by the various experiments appear in general quite compatible with each other in both shape and absolute cross sections, within the experimental uncertainties and within the differences expected (at high p_T) due to the slightly dissimilar c.m. energies of the various measurements (see Sec. IV A). The spectra are characterized by an exponential distribution (with inverse slope ~150 MeV) at low p_T ($p_T \lesssim 1$ GeV/c), followed by a power law with exponent ~10 and then a drop at the highest p_T's when running out of phase space for particle production, approaching the kinematical limit ($p_T^{\rm max} = \sqrt{s}/2 =$ 11–12 GeV/c at midrapidity).

III. INCLUSIVE PION SPECTRA IN p-p COLLISIONS AT $\sqrt{s} \approx 22.4$ GeV: NLO PQCD CALCULATIONS

The inclusive cross section for the production of a single pion, differential in transverse momentum p_T and rapidity y, takes the following form at NLO [24]:

$$\frac{d\sigma}{d\mathbf{p_T}dy} = \sum_{i,j,k=q,g} \int dx_1 dx_2 F_{i/p}(x_1, \mu_F) F_{j/p}(x_2, \mu_F) \times \frac{dz}{z^2} D_k^{\pi}(z, \mu_{ff}) \left[\left(\frac{\alpha_s(\mu_R)}{2\pi} \right)^2 \frac{d\hat{\sigma}_{ij,k}}{d\mathbf{p_T}dy} + \left(\frac{\alpha_s(\mu_R)}{2\pi} \right)^3 K_{ij,k}(\mu_R, \mu_F, \mu_{ff}) \right]. \quad (1)$$

$F_{i/p}$ are the PDFs of the incoming protons p, $D_k^\pi(z, \mu_{ff})$ are the parton-to-pion FFs describing the transition of the parton k into a pion, $d\hat{\sigma}_{ij,k}/d\mathbf{p_T}dy$ is the Born cross section of the subprocess $i + j \rightarrow k + X$, and $K_{ij,k}$ is the corresponding higher-order term (the full kinematic dependence is omitted for clarity). In this paper, we use the INCNLO program [23] to compute the cross sections, supplemented with various PDFs and FF sets (see below). The truncation of the perturbative series at next-to-leading order accuracy in α_s introduces an artificial dependence, with magnitude $\mathcal{O}(\alpha_s^3)$, of the cross section on initial- and final-state factorization scales μ_F and μ_{ff}, as well as on the renormalization scale μ_R. The choice of scales is to a large extent arbitrary. One often uses as a ''standard'' choice the hard scale of the process, e.g. $\mu_R = \mu_F = \mu_{ff} = p_T$. A more theoretically sound solution is given by using the principle of minimum sensitivity [28]. Phenomenological comparisons of pQCD results at various orders (LO, NLO, NNLO) among each other and against various experimental data sets (for charm and beauty, top, Z, W bosons, ...) indicate that choosing a relatively low range of scales $\mu/p_T = 1/3 - 1/2$ provides effectively a reduced sensitivity to higher-order effects [29]. We thus use $\mu_R = \mu_F = \mu_{ff} = p_T/\kappa$, with variation between $\kappa = 2$–3. At small p_T and for the scale $p_T/3$, the factorization scale approaches the starting scale Q_0 of the PDF evolution, where the parton densities are not constrained by data. To avoid this problem, we compute only the pion spectra above[1] $p_T = 3$ GeV/c.

At large values of p_T, the use of the fixed-order perturbation theory is fully justified, since the perturbative series is controlled by a small expansion parameter $\alpha_s(p_T^2)$. However, in the typical kinematic range of fixed-target experiments, where $x_T \equiv 2p_T/\sqrt{s} \gtrsim 0.1$, the coefficients of the perturbative expansion are enhanced by extra powers of logarithmic terms of the form $\alpha_s^n \ln^{2n}(1 - x_T)$ or $\alpha_s^n \ln^{2n-1}(1 - x_T)$. Resummation to all orders of such ''threshold'' terms—which appear because the initial partons have just enough energy to produce the high-transverse momentum parton—have been carried out at next-to-leading logarithmic (NLL) accuracy in [30,31]. These studies confirm that accounting for these terms results in a large (approximately p_T-independent) enhancement of the perturbative cross section for pion production in the range of fixed-target energies of relevance here ($\sqrt{s} \approx 20$ GeV). These studies also find that the scale dependence is also reduced at NLL compared to NLO. The presently used fixed-order calculations (INCNLO) do not include threshold resummations, but their effect in the final spectrum is accounted for, in an effective way, by our choice of relatively small theoretical scales $\mu/p_T = 1/2$–$1/3$, which results in a cross-section increase of a factor of ~2–3 as compared to the $\mu/p_T = 1/2$–2 range used e.g. in [30,31].

The two nonperturbative inputs of Eq. (1) are the parton densities and the fragmentation functions. The former are obtained mainly from global-fit analyses of deep-inelastic electron-proton data, the latter from hadron production results in e^+e^- collisions. The PDFs are known to within ~20% uncertainty [32] in the kinematic range of interest here: $x_T = p_T/p_T^{\max} \approx 0.2$–$0.5$ at midrapidity. We use here two of the latest standard PDFs available: MRST04 [33] and CTEQ6.1M [32]. For the quark and gluon fragmentation functions into pions, we use and compare three parametrizations: the commonly used AKK05 [34] plus two more recent sets DSS [35] and AKK08 [36]. The dominant fragmentation contribution to Eq. (1) comes from the large-z domain: $\langle z \rangle = \langle p_{\text{hadron}}/p_{\text{parton}} \rangle \approx 0.8$ for $p_T \gtrsim 3$ GeV/c at $\sqrt{s} = 22.4$ GeV, where the e^+e^- fragmentation data used to obtain the FFs are scarce. In addition, the gluon-to-pion FF is not well determined by e^+e^- annihilation data, as it appears there only at NLO, and we explore small fragmentation scales (in particular, when using $\mu_{ff} = p_T/3$) far away from the kinematical regions where the e^+e^- fits are performed. All of these issues, which were a concern for the older FF sets like KKP [37], Kre [38] or AKK05, have been partially solved with the most recent fits [25] which include for the first time also hadronic data (and error analyses, such as for HKNS [39]) in their global analyses. These new fits cover a larger z range and are more sensitive to the gluon fragmentation. As a result, the normalization of the gluon fragmentation function into pions is increased by e.g. up to 50% in AKK08 [36] with respect to AKK05 [34] at the Z^0 mass scale. This has an obvious impact in the absolute normalization of the predicted pion spectra as we discuss below.

In Figs. 2 (spectra) and 3 (ratio data/pQCD), the measured pion p-p single inclusive distributions at various energies are compared to the corresponding NLO predictions for varying theoretical scales ($\mu = p_T/3$ and $p_T/2$), PDFs (MRST04 and CTEQ6.1M) and FFs (AKK05, AKK08 and DSS). In general, the calculations tend to underpredict the measured cross sections. The overall agreement, in the p_T dependence and absolute normalization, improves going from the left (scales $\mu = p_T/3$) to the right (scales $\mu = p_T/2$) and when using MRST instead of CTEQ. The MRST04 parametrization results in a cross section 25% larger than using CTEQ6.1M in the range[2] $p_T = 3$–6 GeV/c. Such a difference in the resulting cross sections is larger than expected from error analysis within a single PDF set. The AKK08 and DSS fragmentation func-

[1]Whenever it becomes smaller than the minimum Q_0 allowed by the PDF or FF parametrization, the hard scale Q is frozen at Q_0.

[2]However, closer to the kinematical limit, above 8 GeV/c, the trend changes rapidly and the CTEQ6.1M fit overshoots the MRST04 one by up to 40%, indicating the large current uncertainty of the gluon and sea-quark densities at high values of x.

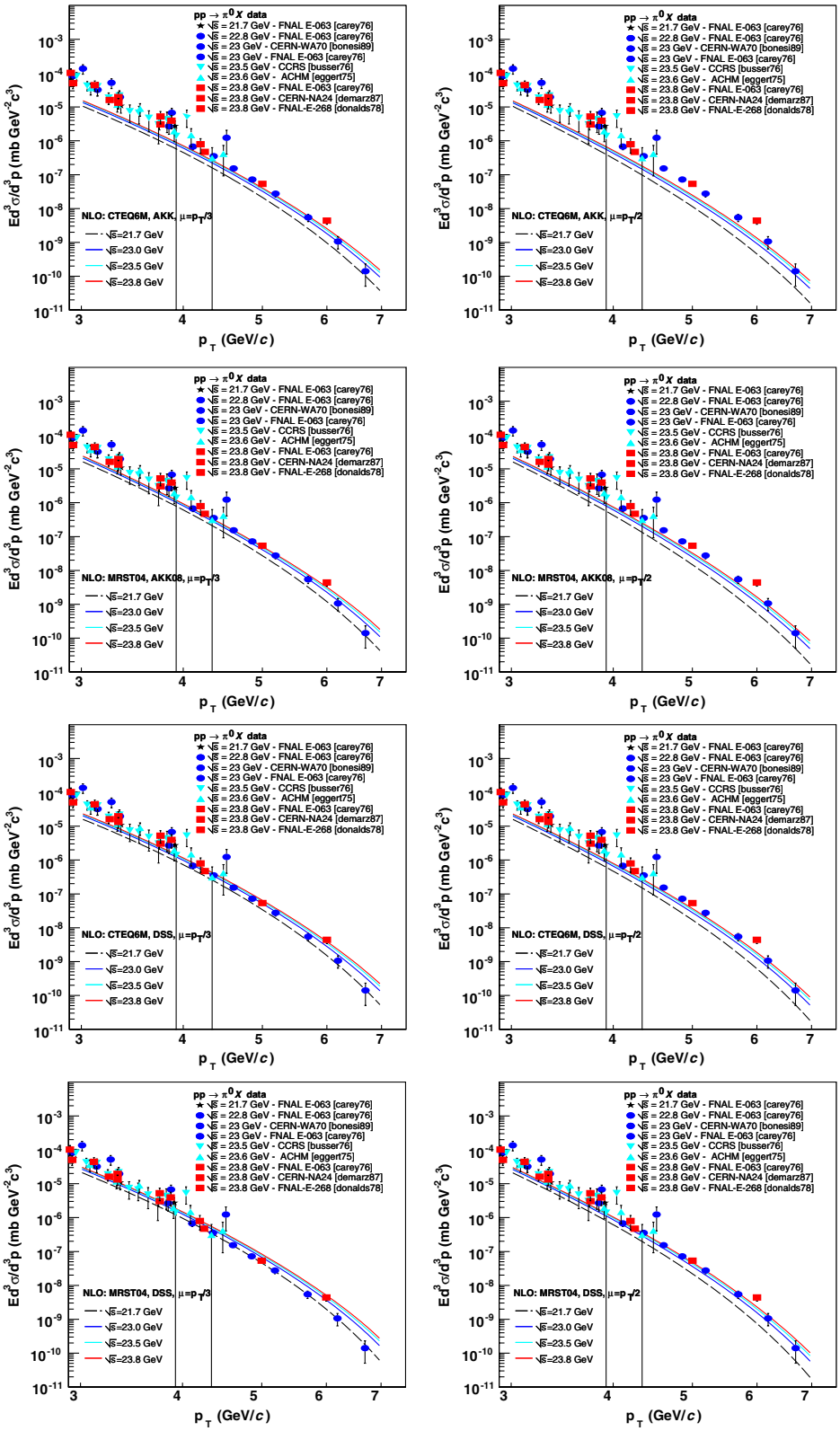

FIG. 2 (color online). Comparison of pion transverse spectra measured in p-p collisions at $\sqrt{s} \approx 21.7$–23.8 GeV to NLO pQCD predictions. The left (right) plots are for theoretical scales $\mu = p_T/3$ ($p_T/2$). Two sets of PDFs (MRST04 and CTEQ6.1M) and three FFs (AKK05, AKK08, and DSS, from top to bottom) are used.

tions reproduce better the data than the AKK05 ones. The overall trend is consistent with MRST04 and AKK08/DSS predicting a *higher* pion yield than CTEQ6.1 and AKK05 in the kinematic range of interest here. In any case, the data-theory agreement at fixed-target energies for high-p_T pions is clearly better than for prompt-photon production,

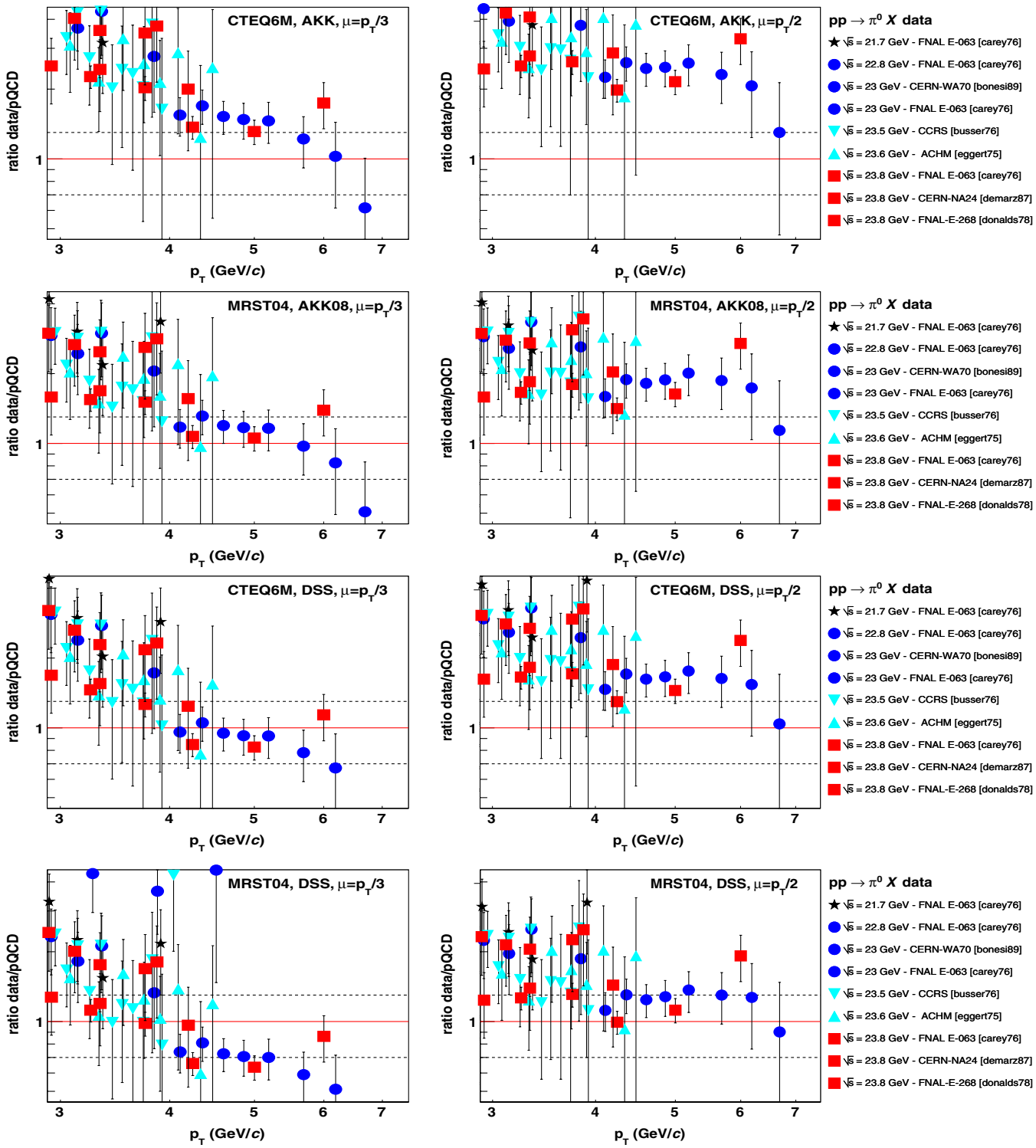

FIG. 3 (color online). Ratio of data over pQCD for pion transverse spectra in p-p collisions at $\sqrt{s} \approx 21.7$–23.8 GeV. The left (right) plots are for theoretical scales $\mu = p_T/3$ ($p_T/2$). Two sets of PDFs (MRST04 and CTEQ6.1M) and three FFs (AKK05, AKK08, and DSS, from top to bottom) are used. The dashed lines are just indicative for variations of $\pm 30\%$ from the reference at $R = 1$.

where the measured E706 yield at $\sqrt{s} = 31.6$–38.6 GeV appears to be 2–3 times larger than the corresponding INCNLO predictions [40].

IV. INCLUSIVE PION SPECTRA IN p-p COLLISIONS AT $\sqrt{s} = 22.4$ GeV: A PRACTICAL PARAMETRIZATION

After verifying that the fixed-order pQCD calculations can reproduce relatively well the existing high-p_T pion data at fixed-target energies, the second motivation of this study is to provide a practical parametrization of the p-p pion spectrum at $\sqrt{s} = 22.4$ GeV to be used as a reference baseline for high-p_T π^0 production in A-A collisions at the same c.m. energy, where no proton-proton data has been yet measured at RHIC [13]. We discuss here the method followed to obtain a fit from the existing experimental data sets after rescaling them to a common center-of-mass energy making use of the NLO predictions.

A. Center-of-mass energy rescaling

The existing data sets (Table I) cover the range of c.m. energies from 21.7 to 23.8 GeV. Although at low p_T (below ~ 2 GeV/c) the small differences in $\sqrt{s}$ result in negligible variations of the soft pion yield and all spectra agree well (see Fig. 1), at high p_T—as one approaches the kinematical limit—a couple of GeV of extra c.m. energy available can result in a significant change in the parton-parton cross sections. For instance, as can be seen in Fig. 4, at $p_T = 5$ GeV/c, going from $\sqrt{s} = 22.4$ GeV up (down) to 23.8 GeV (21.8 GeV) results in an increase (decrease) of the cross section by a factor of $\sim 60\%$ ($\sim 30\%$).

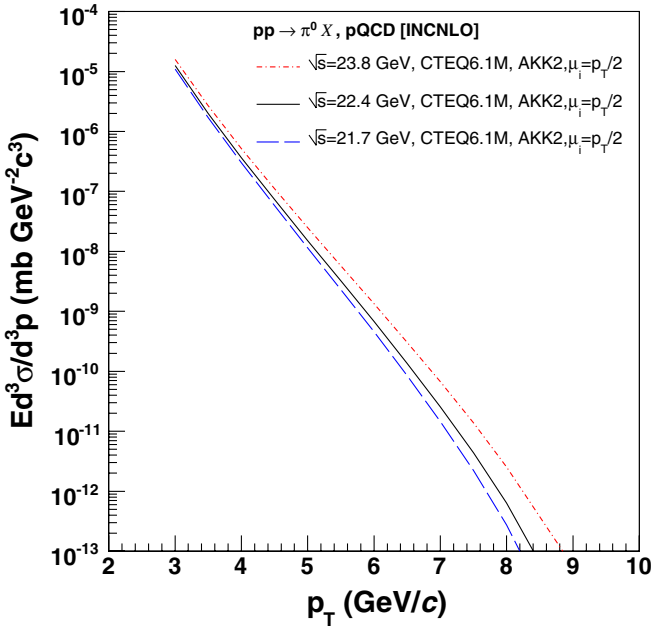

FIG. 4 (color online). Differential π^0 cross sections in p-p collisions predicted by NLO pQCD calculations with scales $\mu = p_T/2$, CTEQ6.1M parton distribution functions, and AKK08 fragmentation functions at $\sqrt{s} = 21.7$, 22.4 and 23.8 GeV.

Although, as seen in the previous section, there are relatively large uncertainties in the NLO predictions for the *absolute* cross sections, most of these uncertainties cancel out when taking *ratios* of the predicted perturbative yields at different, yet close, c.m. energies. In particular, the (large) scale dependence is completely removed. One can, thus, rescale all experimental data points measured at a given $\sqrt{s} = X$ GeV (in the range 21.8–23.8 GeV) to a common $\sqrt{s} = 22.4$ GeV value via the following prescription:

$$\frac{d\sigma_{\rm exp}(\sqrt{s} = 22.4\ {\rm GeV})}{dp_T} = \left(\frac{d\sigma_{\rm NLO}/dp_T(\sqrt{s} = 22.4\ {\rm GeV})}{d\sigma_{\rm NLO}/dp_T(\sqrt{s} = X\ {\rm GeV})}\right) \times \frac{d\sigma_{\rm exp}(\sqrt{s} = X\ {\rm GeV})}{dp_T}. \quad (2)$$

The pQCD cross sections are computed in the range $p_T \approx 3$–10 GeV/c for the 4 energies under consideration, and the ratio over the predictions at $\sqrt{s} = 22.4$ GeV is fitted to a polynomial form of order 2 or 4. Obviously, to minimize the theoretical uncertainties, both the denominator and the numerator of the NLO "rescaling factor" [the expression in parentheses in Eq. (2)] need to be computed using consistently the same PDFs, FFs and scales. The scaling factors provided here are obtained averaging over various different choices of these ingredients. The resulting scaling factors differ, in any case, as expected by a very small factor $\pm 5\%$, well covered within the experimental uncertainties alone. The functional form of the rescaling factor is chosen so that the correction is zero at $p_T = 0$ GeV/c, so as to obtain a smooth extrapolation in the low-p_T region. In any case, below $p_T \approx 1$ GeV/c, the correction is (well) below $\sim 5\%$, and, so, the experimental low-p_T points are virtually unmodified as they should be by applying this rescaling procedure. The final correction functions are shown as a function of p_T in Fig. 5.

In order to better estimate the uncertainty of the rescaling factors computed theoretically, the energy rescaling has also been determined *a posteriori*, assuming that the invariant production cross section is a scaling function of $x_T \equiv 2p_T/\sqrt{s}$:

$$E\frac{d^3\sigma(pp \to \pi X)}{d^3p}(\sqrt{s}) \propto \left(\frac{1}{\sqrt{s}}\right)^4 F(x_T), \quad (3)$$

as it should be in perturbative QCD. Taking for the function F the final parametrization discussed in the next section, $F(x_T) = (22.4\ {\rm GeV})^4 f(x_T \times [11.2\ {\rm GeV}])$, the rescaling factor is computed using Eq. (3). The difference between this empirical estimate and the theoretical rescaling factors, roughly 10%, is assigned as the uncertainty of the present energy rescaling procedure.

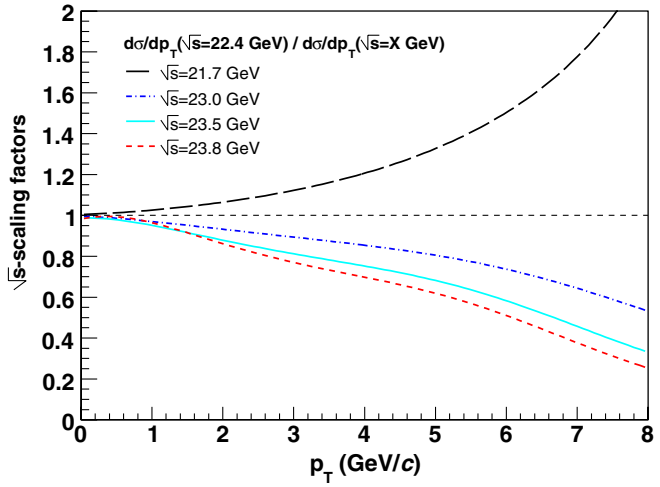

FIG. 5 (color online). Rescaling correction factors of the pion cross sections at c.m. energies 21.7–23.8 GeV to a common $\sqrt{s} = 22.4$ GeV value, as a function of p_T, obtained from the ratio of NLO calculations given by Eq. (2).

B. Global fit of the rescaled pion p_T spectra at $\sqrt{s} = 22.4$ GeV

By applying the appropriate energy correction factors discussed in the previous section to all of the experimental data sets, we obtain a new set of data points which approximates better the expected π^0 spectrum at $\sqrt{s} = 22.4$ GeV. The experimental spectrum $\frac{Ed^3\sigma}{d^3p}|_{y=0}$ is fitted to the following empirical 4-parameter functional form:

$$f(p_T, \{p_i\}_{i=0,3}) = p_0 \cdot [1 + (p_T/p_1)]^{p_2} \cdot [1 - (p_T/p_T^{\max})]^{p_3}. \quad (4)$$

Such a formula interpolates well between the low-p_T exponential shape and the high-p_T power law while fulfilling the requirement of being zero at the kinematical limit ($p_T^{\max} = 11.2$ GeV/c, fixed in the fit). The p_0 parameter gives the cross section at zero p_T, p_1 indicates the transition value from soft to hard production, and the p_2 and p_3 exponents characterize the power-law and end of phase-space ranges. After rejecting two data sets which are not consistent with the rest of spectra (see below), we obtain a final set of $n_{\rm dat} = 194$ data points fitted with Eq. (4). The resulting fit is shown in Fig. 6. The parameters are obtained from the minimization of the χ^2 function

$$\chi^2(\{p_i\}) = \sum_{j=1}^{n_{\rm dat}} \left[\frac{\frac{Ed^3\sigma}{d^3p}|_{y=0}(p_{T_j}) - f(p_{T_j}, \{p_i\})}{\sigma_j} \right]^2, \quad (5)$$

where σ_j is the statistical and systematic error of point j added in quadrature. The error of the parameters p_i is given from a deviation of $\Delta\chi^2$ from its minimum:

$$\chi^2(\{p_i + \delta p_i\}) - \chi^2(\{p_i\}) = \Delta\chi^2. \quad (6)$$

Although a usual choice is $\Delta\chi^2 = 1$, we shall conservatively allow for a larger variation of the fit parameters assuming $\Delta\chi^2 = 50$ in what follows,[3] similarly to what is done in global-fit analyses of parton densities or fragmentation functions (see e.g. [35,41]). From this procedure, the corresponding parameters are

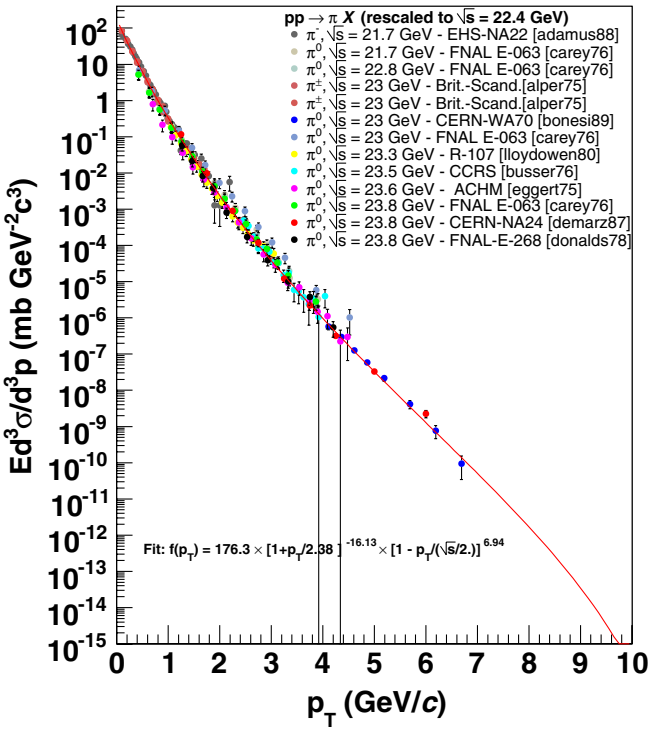

FIG. 6 (color online). Compilation of all pion transverse spectra measured in p-p collisions at $\sqrt{s} = 21.7$–23.8 GeV, rescaled to a common $\sqrt{s} = 22.4$ GeV energy, as discussed in the text, and fitted to Eq. (4), with the parameters (7).

$$\begin{aligned} p_0 &= 176.3 \pm 69.7\ [\text{mb GeV}^{-2}\, c^3], \\ p_1 &= 2.38 \pm 1.19\ [\text{GeV}/c], \\ p_2 &= -16.13 \pm 7.21, \\ p_3 &= 6.94 \pm 5.64, \qquad \chi^2/\text{ndf} = 208.2/190, \end{aligned} \quad (7)$$

with an important correlation between parameters and errors, as indicated by the large nondiagonal terms of the covariance (error) matrix V_{ij}:

$$V_{ij} = \begin{pmatrix} 1.000 & -0.725 & -0.603 & 0.394 \\ -0.725 & 1.000 & 0.981 & -0.862 \\ -0.603 & 0.981 & 1.000 & -0.940 \\ 0.394 & -0.862 & -0.940 & 1.000 \end{pmatrix}.$$

Note that at low p_T this fit is consistent with an exponentially decreasing function with inverse slope $-p_1/p_2 = 148 \pm 16$ MeV. The scale p_1, which naively separates soft from hard dynamics, has a sensible value

[3]This would correspond to an increase of 25% of $\chi^2_{\rm min}/\text{ndf}$, with ndf $\simeq 200$.

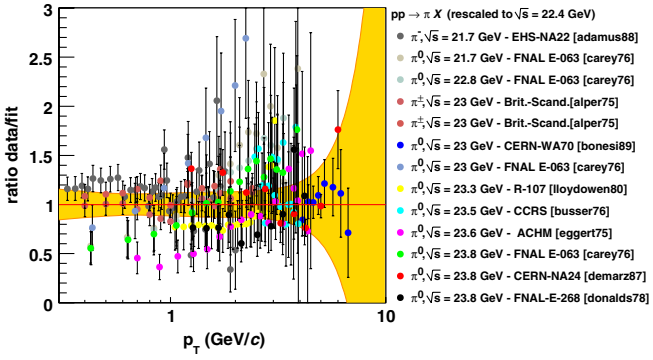

FIG. 7 (color online). Ratio of all pion transverse spectra measured in p-p collisions rescaled to $\sqrt{s} = 22.4$ GeV over the fit given by Eq. (4) with the parameters (8). The yellow band represents the uncertainty assigned to the parametrization, as given by Eq. (7). The [carey76] and [eggert75] points at $\sqrt{s} =$ 23.6 and 23 GeV, respectively [14,20] have been excluded from the global fit.

$\sim$2–3 GeV. Finally, the negative power slope $p_2 = -16.13$ is found to be larger in absolute value than $p_2 = -10$ obtained at $\sqrt{s} = 200$ GeV [42]. This is expected from the steeper dependence of parton densities and fragmentation functions probed at higher x and z, respectively, at lower $\sqrt{s}$. The uncertainty Δf of the fit is given by

$$\Delta f = \left[\sum_{i,j=0}^{3} \frac{\partial f}{\partial p_i} V_{ij} \frac{\partial f}{\partial p_j} \right]^{1/2}. \tag{8}$$

The relative uncertainty of the parametrization $\Delta f/f$ spans the range from $\sim$15% at low $p_T \lesssim 2$ GeV/c up to 25% (40%) at $p_T = 4$ GeV/c (5 GeV/c) in the range covered by the RHIC measurements [13]. At higher p_T's the fit is completely unconstrained due to the lack of data, and its uncertainty is very large.

Figure 7 shows the ratio of all data sets compiled and rescaled in this work over the fit Eq. (4) with the parameters quoted above. All data sets—but Carey76 [14] at $\sqrt{s} =$ 23 GeV and Eggert75 [20] at $\sqrt{s} = 23.6$ GeV which have a shape and absolute normalization inconsistent with the rest of measurements and have not been included in the final global analysis—show a rather good agreement with the proposed parametrization, as also indicated by $\chi^2/\mathrm{ndf} \simeq 1.1$. We note that our empirical fit includes also the low-p_T range, not amenable to perturbative analysis, since we want to provide a (potentially useful) p-p reference parametrization in the whole range covered by the nucleus-nucleus data.

V. SUMMARY

We have compared the available high-p_T pion spectra measured in proton-proton collisions in the range $\sqrt{s} =$ 21.7–23.8 GeV (CERN-ISR collider and CERN and FNAL fixed target) to next-to-leading order pQCD calculations with recent PDFs and FFs. A choice of the theoretical (factorization, fragmentation and normalization) scales between $p_T/3$ and $p_T/2$ reproduces well the magnitude and shape of the experimental data. CTEQ6.1 and MRST04 parton densities yield results different by up to 25%. Second-generation parton-to-pion FFs with updated constraints on the gluon and large-z fragmentation region, such as DSS or AKK08, improve the agreement of the data with the calculations compared to older FF parametrizations.

A baseline nucleon-nucleon reference p_T distribution for inclusive π^0 production at $\sqrt{s} = 22.4$ GeV has been determined from a global-fit analysis of the available data. The measured (high-p_T) data sets have been rescaled at a common c.m. energy making use of the predicted NLO pQCD yields at the various $\sqrt{s}$. The resulting parametrization is consistent within $\pm$15% and $\pm$40% systematic uncertainty with the rescaled π^0 and $\pi^{\pm}$ measurements at low ($p_T \lesssim 2$ GeV/c) and moderate ($p_T \simeq 5$ GeV/c) transverse momentum. Such a reference—Eq. (4) with fit parameters (7)—can be used in order to obtain the nuclear modification factor of high-p_T pion production in A-A collisions at $\sqrt{s_{NN}} = 22.4$ GeV measured at RHIC.

ACKNOWLEDGMENTS

Valuable comments and discussions with Klaus Reygers and Mike J. Tannenbaum are acknowledged. We thank Simon Albino for providing us with the latest AKK08 fragmentation functions. D. d'E. is supported by the 6th EU Framework Program (Contract No. MEIF-CT-2005-025073). F. A. thanks the hospitality of the CERN PH-TH department where part of this work has been completed.

[1] W. M. Geist, D. Drijard, A. Putzer, R. Sosnowski, and D. Wegener, Phys. Rep. **197**, 263 (1990).
[2] D. d'Enterria, "High-p_T Hadrons and Jets in High-Energy Heavy-Ion Collisions," Lect. Notes Phys. (Springer-Verlag, Berlin, to be published).
[3] G. Bunce, N. Saito, J. Soffer, and W. Vogelsang, Annu. Rev. Nucl. Part. Sci. **50**, 525 (2000).
[4] B. Jager, A. Schafer, M. Stratmann, and W. Vogelsang, Phys. Rev. D **67**, 054005 (2003).
[5] S. S. Adler *et al.* (PHENIX Collaboration), Phys. Rev. Lett. **91**, 072301 (2003).
[6] J. Adams *et al.* (STAR Collaboration), Phys. Rev. Lett. **91**,

172302 (2003).
[7] R. Baier, D. Schiff, and B. G. Zakharov, Annu. Rev. Nucl. Part. Sci. **50**, 37 (2000).
[8] M. Gyulassy, I. Vitev, X. N. Wang, and B. W. Zhang, arXiv:nucl-th/0302077.
[9] T. Isobe, Acta Phys. Hung. A **27**, 227 (2006).
[10] B. I. Abelev *et al.* (STAR Collaboration), Phys. Lett. B **655**, 104 (2007).
[11] C. Blume, Nucl. Phys. **A783**, 65 (2007), and references therein.
[12] D. d'Enterria, Phys. Lett. B **596**, 32 (2004).
[13] A. Adare *et al.* (PHENIX Collaboration), Phys. Rev. Lett. **101**, 162301 (2008).
[14] D. C. Carey *et al.*, Phys. Rev. D **14**, 1196 (1976).
[15] M. Bonesini *et al.* (WA70 Collaboration), Z. Phys. C **38**, 371 (1988).
[16] C. De Marzo *et al.* (NA24 Collaboration), Phys. Rev. D **36**, 8 (1987).
[17] G. Donaldson *et al.*, Phys. Lett. **73B**, 375 (1978).
[18] D. Lloyd Owen *et al.*, Phys. Rev. Lett. **45**, 89 (1980).
[19] F. W. Busser *et al.*, Nucl. Phys. **B106**, 1 (1976).
[20] K. Eggert *et al.*, Nucl. Phys. **B98**, 49 (1975).
[21] B. Alper *et al.* (British-Scandinavian Collaboration), Nucl. Phys. **B100**, 237 (1975).
[22] M. Adamus *et al.* (EHS-NA22 Collaboration), Z. Phys. C **39**, 311 (1988).
[23] P. Aurenche, T. Binoth, M. Fontannaz, J.-P. Guillet, G. Heinrich, E. Pilon, and M. Werlen, http://lappweb.in2p3.fr/lapth/PHOX_FAMILY/readme_inc.html.
[24] P. Aurenche, M. Fontannaz, J. P. Guillet, B. A. Kniehl, and M. Werlen, Eur. Phys. J. C **13**, 347 (2000).
[25] S. Albino *et al.*, arXiv:0804.2021, and references therein.
[26] http://durpdg.dur.ac.uk/HEPDATA/.
[27] D. d'Enterria, J. Phys. G **31**, S491 (2005).
[28] P. M. Stevenson, Phys. Rev. D **23**, 2916 (1981); P. M. Stevenson and H. D. Politzer, Nucl. Phys. **B277**, 758 (1986); P. Aurenche, R. Baier, M. Fontannaz, and D. Schiff, Nucl. Phys. **B286**, 509 (1987).
[29] A. Geiser, Nucl. Phys. B, Proc. Suppl. (unpublished).
[30] D. de Florian and W. Vogelsang, Phys. Rev. D **71**, 114004 (2005).
[31] D. de Florian, W. Vogelsang, and F. Wagner, Phys. Rev. D **76**, 094021 (2007).
[32] J. Pumplin *et al.* (CTEQ Collaboration), J. High Energy Phys. 07 (2002) 012.
[33] A. D. Martin, R. G. Roberts, W. J. Stirling, and R. S. Thorne, Phys. Lett. B **604**, 61 (2004).
[34] S. Albino *et al.*, Nucl. Phys. **B725**, 181 (2005); **B734**, 50 (2006).
[35] D. de Florian, R. Sassot, and M. Stratmann, Phys. Rev. D **75**, 114010 (2007).
[36] S. Albino, B. A. Kniehl, and G. Kramer, Nucl. Phys. **B803**, 42 (2008).
[37] B. A. Kniehl, G. Kramer, and B. Pötter, Nucl. Phys. **B582**, 514 (2000).
[38] S. Kretzer, Phys. Rev. D **62**, 054001 (2000).
[39] M. Hirai, S. Kumano, T. H. Nagai, and K. Sudoh, Phys. Rev. D **75**, 094009 (2007).
[40] P. Aurenche, M. Fontannaz, J. P. Guillet, E. Pilon, and M. Werlen, Phys. Rev. D **73**, 094007 (2006).
[41] J. Pumplin *et al.*, Phys. Rev. D **65**, 014013 (2001).
[42] S. S. Adler *et al.* (PHENIX Collaboration), Phys. Rev. Lett. **91**, 241803 (2003).